DOI: 10.13009/EUCASS2025-118
11TH EUROPEAN CONFERENCE FOR AERONAUTICS AND SPACE SCIENCES (EUCASS)

An overview of ignition systems within Students' Space Association sounding rockets

Michał Kret†, Bartosz Dąbrowski*, Bartosz Hyży*, Szymon Krupa*, Piotr Łyżwa*, Remigiusz Michna*, Michał Tomporowski*, Jędrzej Chrostowski*, Michał Krajewski* and Szymon Życiński**

Students' Space Association, Faculty of Power and Aeronautical Engineering Warsaw University of Technology

Institute of Heat Engineering, Nowowiejska 21/25, 00-665 Warsaw, Poland

michal.kret.stud@pw.edu.pl
† Corresponding Author

Abstract
Ignition systems play a pivotal role in the rocket motors design process, impacting every stage of engine performance and, as a consequence, prospectively successful flight. Despite the simplicity of both construction and operation, work on igniters often generates difficulties. The main one being the prediction of their performance, which requires the usage of complex mathematical models.
The Rocketry Division of the Students' Space Association at Warsaw University of Technology has been developing sounding rockets for more than ten years now. Each of the nine flight-tested rockets was propelled by motors developed internally along with igniters. The principal objective of this presentation is to picture the variety of ignition systems solutions developed and tested over a span of the past decade within the Association.

1. Introduction

Students' Space Association (SKA – in polish Studenckie Koło Astronautyczne) at Warsaw University of Technology was founded in 1996. Currently it gathers nearly two hundred members, focused on developing projects related to space technologies, such as Martian rovers, sounding rockets, nano satellites, and stratospheric balloons. Among the greatest achievements of the Association are: the development and launch of the first Polish satellite PW-SAT 1 [1], setting the record of flight apogee of a Polish amateur sounding rocket [2], and numerous trophies from rover challenges across the world.

The Rocketry Division was established in 2009, with the beginning of the first project, the Amelia 1 rocket - a single stage rocket, propelled by a solid motor, with apogee of 500 m [3]. After the success of the first project, the next ones, with more ambitious goals, followed. To this day the Division has successfully designed and flight tested nine sounding rockets (presented in Figure 1), eight of them were propelled by a solid rocket motor, while the Twardowsky rocket was the first hybrid rocket developed at Warsaw University of Technology [4]. Currently, team members are developing the second hybrid rocket, successor of Twardowsky 1 - Twardowsky 2, with hope of participating in students' team competitions such as EuROC or Spaceport America Cup.

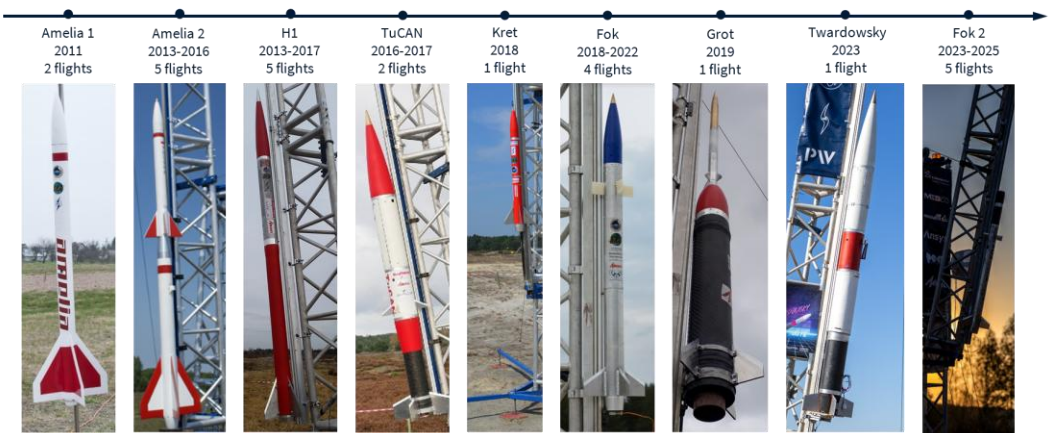

Figure 1 Timeline of sounding rockets developed by Students' Space Association

DOI: 10.13009/EUCASS2025-118

Since the beginning, the fundamental design principle was to develop and qualify each rocket subsystem in-house, especially the propulsion subsystems, with help of university academics. This approach allowed the members to gather valuable knowledge and experience; however, the limited resources made it difficult to conduct large-scale test campaigns. To further expand the testing possibilities, especially conducting the static fire tests, the HFSTS project was started in 2022, providing the necessary test environment [5].

One of the main challenges faced during the design phase of each rocket motor was the igniter. The complexity of physical phenomena occurring during combustion poses challenge in mathematical modelling and enforces specific requirements to mechanical design. On the other hand, cruciality of this component requires repeated testing to prove the reliability in motor ignition. With development of each new motor, the designed igniters have improved, basing on the knowledge gained. The expansion from solids to hybrids has also broadened the range of used materials and design solutions. This paper presents the summary of ignition system heritage built in Students' Space Association, along with experimental data gathered during these systems' development.

2. Physical and mathematical modelling of propellant ignition

Due to different characteristics of combustion process and grain regression in solid propellant rocket motors and hybrid rocket engines, the ignition processes occur differently. The main goal of igniter design should be the same, to obtain stable, quick, and repeatable ignition of the motor.

2.1. Ignition in solid propellant motors

In their work d'Agostino et al. [6] state that the ignition process can be divided into three stages, consisting of complex transient events, which take place between sending the activation signal to the igniter, to when the motor is fully ignited. The first stage is the induction period before first local ignition of propellant grain surface. Heat flux generated from the ignition charge combustion increases the propellant grain surface temperature and diffuses deeper into material [7]. It is assumed that during this phase no chemical reactions take place [8], and the pressure is constant after the initial increase from the ignition mass charge combustion [6]. After sufficient temperature on the grain surface is reached, chemical reactions leading to binder pyrolysis and oxidiser decomposition begin to occur. Further supply of the heat leads to flame formulation and self sustainability of the propellant combustion [8]. As the flame continues to spread, a rise in combustion chamber pressure is observed with maximum occurring when the chamber is filled with flame [6].

Over the years of study multiple theories have been brought forward. However, experimental data from laboratory tests rarely were not sufficiently accurate and reliable to properly validate proposed models [9]. As ignition process consists of series of transient phenomena and depends on propellant and ignition charge material properties, it is difficult to formulate a universally adequate model.

2.1.1. Solid phase thermal theory

The first analytical model applicable to solid propellant ignition is attributed to Hicks [10], who assumed a semi-infinite slab or rod of constant density material, bounded by a plane face, which is also a source of heat flux. Therefore, this model does not take into consideration mass diffusion, nor the gas phase, which is a result of grain surface regression. Basing on these assumptions, a transient heat exchange partial differential equation can be formulated [10]:

$$c\frac{\partial T}{\partial t} - \lambda\frac{\partial^2 T}{\partial x^2} - Q = 0;\; x \geq 0, t > 0 \tag{1}$$

Where c is the heat capacity per unit of volume, λ is thermal conductivity, x is distance measured from propellant surface and Q is the rate of heat evolution per unit of volume. The last term can be expressed as rate of reaction of zero order with Arrhenius formula (see equation (2)) [10].

$$Q = qC_f C_o A\, exp\left(-\frac{E}{RT}\right) \tag{2}$$

DOI: 10.13009/EUCASS2025-118

Where q is the enthalpy of reaction per unit of volume, C_f, C_o are the fuel and oxidisers concentrations, A is pre-exponential factor, E is the reaction activation energy and R is the gas constant. On the outer surface of analysed rod (x=0), it is assumed, that the heat is transferred by convection, governed by equation (3).

$$-\lambda \frac{\partial T}{\partial x} = \alpha\left(T_g - T\right) \tag{3}$$

Where T_g is the temperature of gaseous combustion products and α is the heat transfer coefficient between them and the grain surface. The second boundary condition at infinity assumes, that the temperature gradient tends to zero, as sources of heat are too far away. To finish formulating the problem, a constant initial temperature is assumed. The basic heat transfer equation governing the ignition can be expanded, to include additional factors as surface regression, radiative heat exchange, or change in concentration of reactants [11]. A number of simplifying assumptions undertaken to form this model are its main weakness [11], [12]. Experiments have proven that in ignition of solid rocket motors participation of gas phase species from propellant vaporization, chemical kinetics, radiative heat transfer, dependency of material properties with temperature and diffusion play a huge part, therefore should not be omitted.

2.1.2. Gas phase theory

Gas phase-based theories have been developed in answer to the drawbacks of solid phase model. First model of gas phase solid propellant ignition was put forward by McAlevy, Cowan and Summerfield, who suggested the theory of one-dimensional, composite solid propellant ignition exposed to conductive heating from a gaseous source, based on results of shock tube experiments [13]. They assumed, that the entirety of heat is generated by a second order reaction between the vaporized fuel binder and oxygen in the atmosphere, not the oxidiser. This heat is transferred to the propellant surface by means of conduction only. The propellant grain starts to vaporize at a constant rate, up to the moment of ignition [11], [12] [13]. The equation governing the heat transfer and heat rate are the same as in Hicks model, however a mathematical criterion of ignition was added:

$$\frac{\partial T}{\partial t} = 0 \tag{4}$$

Equation (4) constitutes a statement that ignition shall occur when the chemical heat generation becomes equal to the conductive heat loss [13]. From that on, formulas for fuel concentration C_f (5) and temperature (6) can be derived :

$$C_f(x,t) = 2\frac{\nu\rho_f A\, exp\left(-\frac{E}{RT}\right)}{\sqrt{D_{fg}}}\sqrt{t}\; ierfc \tag{5}$$

$$T(x,t) = T_s + (T_5 - T_s)erf\left(\frac{x}{2\sqrt{D_{fg}t}}\right) \tag{6}$$

Where v is the volumetric fraction of fuel in propellant, T_s is the temperature on the surface, T_5 is the temperature of quasi-steady uniform state of shock tube, D_{fg} is the heat diffusivity, erf is gauss error function and $ierfc$ is its complementary function. Basing on those two equations a formula for a minimum time - after which at some point along the propellant thickness the ignition condition is fulfilled - can be formulated:

$$t_{min} = KC_o^{-\frac{2}{3}} \tag{7}$$

Where K is a constant dependent on the propellant properties and operating conditions in the shock tube [12] [13].
Further work on gas phase ignition model can be attributed to Hermance et al. [14]. The model was based on assumptions very similar to the ones made in McAlevy work, however, Hermance model considers two different limiting cases of fuel vaporization and includes depletion of reactants [12]. The mass and thermal diffusion rates are equal in Hernace model. Also a different ignition condition was presumed, defined as the achievement of a temperature equal to initial temperature multiplied by factor greater than one; ignition occurs if this condition is fulfilled at any

DOI: 10.13009/EUCASS2025-118

place in the gas phase [14]. Comparing to McAlevy criterion, this time was greater than time at which the temperature – time reversal criterion was fulfilled [12].

2.1.3.Hypergolic and heterogenous ignition

Another theory worth mentioning is the theory of hypergolic ignition, in which exothermic reactions start spontaneously when reactants are brought into contact [12]. Heat generated in those reactions leads to increase in grain surface temperature, exceeding temperature necessary to sustain propellant burning. This model offers an explanation for the effect of gaseous environment on propellant ignition [11]. One dimensional model was proposed by Anderson and Brown [15], based on similar assumptions as previous models, with source of heat from hypergolic reaction and solution of heat and mass transfer equations in solid, condensed and gas phase [12]. Since this model does not have a steady state solution, there are significant difficulties in definition of ignition criterion.

On the basis of hypergolic ignition theory, heterogenous ignition theory was proposed. It is suggested that heat generated in ignition charge combustion increases the temperature of propellant surface to begin oxidiser decomposition reaction, which products come in contact with fuel to start exothermic reaction leading to ignition. It is argued, that at lower pressures or for certain binders' time to ignition is dependent on oxidiser concentration and pressure in similar manner as in hypergolic theory. This theory, despite the fact that some of the sources postulate its veracity, is met with criticism, claiming that the evidence supporting it is burdened with subjective assumptions aimed at obtaining a predetermined result [12].

2.1.4. Empirical models

A more useful approach in igniter system design are models, which allow to estimate the mass of ignition charge, basing on motor properties. One particular model, which was found to be a reliable tool to evaluate mass of charges used not only in motor ignition, but also in pyrotechnic valves and release mechanisms, was presented in NASA report [11]. It relates pressure generated during combustion with initial mass, basing on ideal gas law. Formula is presented in equation (8).

$$p = p_a + \frac{\rho}{\rho - \Delta}\Delta\lambda G \tag{8}$$

Where p_a is the ambient pressure, ρ is the density of ignition material, Δ, called packing density, is a ratio of ignition charge mass (m_c) to chamber free volume (V_c). G is fraction of burned material, λ is energy per unit of mass generated during combustion and is obtained experimentally [11]. Substituting $G = 1$, and transforming equation (8), formula for charge mass is obtained:

$$m_c = \frac{\rho V_c(p_{max} - p_a)}{\rho\lambda + p_{max} - p_a} \tag{9}$$

Where maximum pressure generated during combustion is usually set equal to a value ranging from 0,3 to 0,5 engine operating pressure. As the exact value of λ depends on ignition charge composition, and is unknown during the design process, mass obtained from this equation is usually increased by a margin of at least 10%.

2.2. Ignition in hybrid rocket engines

Hybrid rocket engine ignition process can be divided into four stages: inert heating, ignition, flame propagation, and rapid pressure buildup. In the first stage the solid fuel is heated from the initial temperature to the pyrolysis point. When the temperature of fuel surface reaches the pyrolysis temperature, the pyrolyzed fuel is blown off by the oxidiser and they mix with each other. Then, the flame spreads along the grain surface. The heat flux reaches a balance due to boundary layer structure blocking heat transfer to grain surface; the mass flow rate increases which results in rapid pressure buildup. When pressure in the combustion chamber stabilizes, the ignition process can be considered completed [16].

It is assumed that ignition occurs when the surface temperature of the grain exceeds the ignition temperature. With that assumption, the ignition time and mass flow rate can be calculated.

DOI: 10.13009/EUCASS2025-118

If presumed that axial temperature gradient is negligible; the fuel thermal properties are constant; the grain wall thickness is greater than temperature profile penetration depth; and all solid phase reactions related to fuel vaporization happen in a thin layer adjacent to the regressing surface; heat diffusion equation can be formulated as (10) [17][18].

$$\frac{\partial \mathrm{T}}{\partial t} = \alpha_f \left(\frac{\partial^2 T}{\partial^2 r^2} + \frac{1}{r}\frac{\partial T}{\partial t} \right) \tag{10}$$

Where T is the temperature of grain surface, r is the inner radius of fuel grain. Thermal diffusivity of fuel α_f is given by equation (10)(11).

$$\alpha_f = \frac{K_f}{\rho_f c p_f} \tag{11}$$

K_f, ρ_f and cp_f are the thermal conductivity, density, and specific heat of the fuel grain. For semi-infinite region problem both Dirichlet and Neumann boundary conditions can be used [19]. The second boundary condition is obtained from energy equation. The heat flux delivered by igniter has to provide enough energy to heat up and vaporize the layer of fuel. [17].

$$\dot{Q}_\iota = \rho_f c p_f \dot{r}(t) \left(\frac{\partial T}{\partial t} \right)_1 - K_f \left(\frac{\partial T}{\partial r} \right)_1 \tag{12}$$

Q_i is igniter provided heat flux, $\dot{r}(t)$ is fuel grain radial regression rate and subscript 1 refers to the point on the thin layer where reaction occurs. Due to the character of pyrolysis reaction the regression rate can be expressed by Arrhenius law [18]:

$$\dot{r}(t) = A\, exp \left(\frac{-E_a}{R_g T_1} \right) \tag{13}$$

Where A is pre-exponential factor, E_a is the reaction activation energy and R is specific gas constant. By solving the above equations, using theoretical and experimental data, it is possible to determine the optimum temperature of solid grain surface and oxidiser to fuel ratio for ignition. Also, the ignition delay time can be estimated using these optimized parameters [16].

2.3. Simulation of igniters and ignition in Students' Space Association

The ignition is also one of the elements simulated by the program Rocket Propulsion Analysis Tool (RPAT) developed in-house by the Association. Two main elements have been implemented – igniters and ignition delay. The igniters were introduced in two models: NASA igniter model, influencing the initial conditions of the system, and the more advanced alternative of igniter simulated as a grain-like structure. NASA model is implemented as a jump in pressure (as presented in Figure 2), which in turn influences the initial mass flow rate.

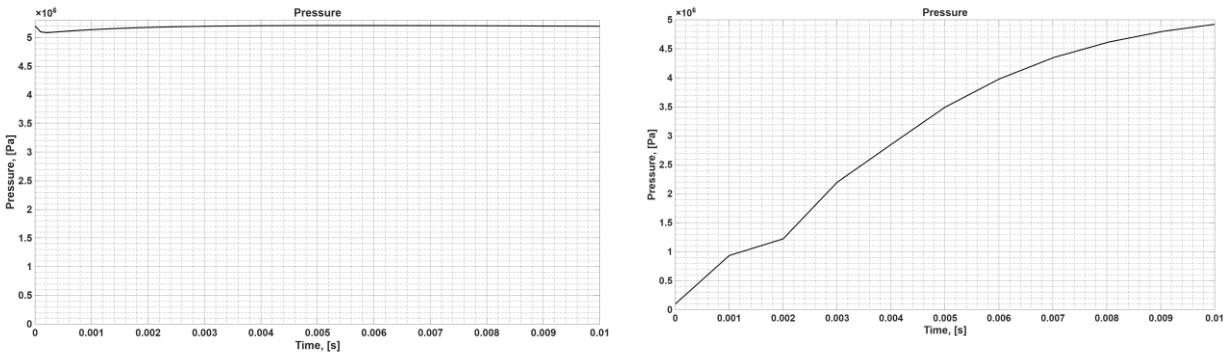

Figure 2 The pressure graph for first 0.01 s of A2 engine simulation with (left) and without (right) applied igniter pressure increase before the simulation start

DOI: 10.13009/EUCASS2025-118

As a result of igniter pressure increase, the model starts calculations from high pressure in comparison to ambient conditions. Due to that, at the start, the change in pressure due to difference between the mass flow rate exiting through the nozzle and the one produced by the fuel combustion can be relatively high if the time step is not chosen carefully, as it is linearly dependent on it. As a result, in the first time step, the model can diverge to the state it would reach by igniting from ambient conditions. To prevent it, the required time step in the case of igniter use is much lower in the beginning phase of the burn. Additional problem of such simplification is the inability to include the influence of shape and time of the igniter burning.

To alleviate the shortcomings of the simple model the igniter can be simulated in a way similar to propellant grain [20]. The igniter can then be burned as object with specified geometry and fuel type, gradually increasing the pressure in the chamber. The produced mass flow merges with the flow from the burning grain, thus the simulation case is similar to the burning of multiple grains with distinct fuels. This is realised by first obtaining the general molar mass of the exiting gases as a mass weighted average of the component gases being at that time present in chamber. The adiabatic constant is then determined from the masses and molar masses of the component gases. The burning process is therefore simulated as grains with different burn law coefficients that produce final mass flow of combined characteristics of the components. Since the igniter charge burns much quicker than the typical grain, in the initial phase of the burn its effect is more pronounced and later disappears completely.

However, this model does not include the even more transient effects that come with igniting the grain such as gradual diffusion of the igniter into the grain at the beginning of the burn. Thus, the total impulse calculated using this method would be smaller than experimental value. The solution for this would be further expansion of physical model.

3. Pyrotechnical materials

Pyrotechnical materials are widely utilized in the aerospace industry for the ignition of both solid and hybrid rocket motors due to their ability to deliver rapid, high-temperature, and to guarantee reliable combustion. Among the numerous compositions developed, three types are most relevant in ignition systems: black powder (BP), boron–potassium nitrate (BPN), and thermite-type formulations. These compositions have been standardized across various aerospace applications due to their favourable ignition reliability, scalability, and relative stability under transport and storage conditions.

Black powder (BP) is a classical pyrotechnic composition consisting of potassium nitrate, charcoal, and sulphur [21]. It is valued for high gas production, and fast deflagration. Despite its age, black powder remains in use, particularly in initiator systems and as a primary ignition charge. However, its drawbacks include relatively low energy density and substantial residue after combustion, which may pose a problem in enclosed systems.

$BKNO_3$ (BPN, boron–potassium nitrate) is a widely used pyrotechnic mixture in aerospace-grade igniters, offering high flame temperatures and rapid energy release. The typical formulation comprises 28% boron and 72% potassium nitrate by mass. The mixture burns with low smoke output and is effective in initiating composite and metallic propellants. The reactivity of boron-based compounds is influenced by the particle size and purity of the ingredients used [22], making it suitable for precise ignition applications, including missile, and sounding rocket motors.

Thermite-based compositions involve a metal fuel, commonly aluminium, reacting with a metal oxide such as iron(III) oxide or copper(II) oxide. These reactions generate extremely high temperatures and molten products, which can be advantageous in igniting insensitive propellants or thermally shielding materials. Industrial variants such as $Al–Fe_2O_3$ and Al–CuO differ in burn rate and light intensity, with nanoscale aluminium significantly enhancing reactivity. Due to their exothermic nature and ability to produce hot slag without huge number of gaseous products, thermite mixtures are sometimes used in pyrogen igniters or as secondary boosters in multi-stage ignition trains [23] [24].

Over the years, the Students' Space Association (SKA) has employed a variety of pyrotechnic compositions in the development and testing of rocket motor ignition systems. The selection of materials was influenced by performance requirements, safety, cost, and availability. The most commonly used compositions included black powder, $BKNO_3$, potassium nitrate–sugar mixtures, and Visco fuse.

Black powder was the most frequently used composition in both solid and hybrid motor igniters, primarily due to its simplicity, availability, and reliability. It was used either as loose powder or pressed into dedicated containers. Despite its relatively low energy density, black powder ensured rapid gas generation and reliable flame propagation, which were especially useful in small motor applications. Its main limitations included sensitivity to moisture and considerable residue after combustion, occasionally leading to clogging of igniter components.

$BKNO_3$ (boron–potassium nitrate) was used in selected igniter designs requiring higher ignition temperatures and more energetic output. Industrial-grade $BKNO_3$ mixtures were favoured for initiating composite propellants, especially

DOI: 10.13009/EUCASS2025-118

where black powder lacked the necessary thermal output or flame intensity. Due to its clean burn and high performance, $BKNO_3$ was typically used in motors with larger grain surface area or less sensitive propellant formulations.

Potassium nitrate–sugar mixtures, commonly known as "caramel propellants," were employed primarily in early hybrid igniter designs. These compositions were simple to manufacture and shape into specific geometries, offering moderate energy output and a long, stable burn. The most common oxidiser-to-fuel ratio ranged between 60:40 and 65:35 by mass. While these mixtures proved useful in initial design iterations, their limitations in ignition reliability and combustion consistency led to their replacement with more predictable compositions in later projects.

Visco fuse, a commercially available slow-burning fuse composed primarily of black powder encased in a protective coating, was also used in SKA projects. It served as both a timing element and direct ignition source. In hybrid motors, visco fuse was glued to the forward face of the fuel grain to ensure consistent ignition across the grain surface. This method allowed for easy adjustability of charge mass and improved reliability compared to earlier configurations using pressed charges or composite initiators.

Together, these compositions enabled flexible and scalable ignition system designs tailored to various motor configurations developed within the Association, from small-scale solid boosters to complex hybrid propulsion systems.

4. Igniters of solid propellant motors

To properly present the topic of igniters design, one should begin with the description of solid rocket motors for which the igniters were intended for. Typical solid propellant motor design has been consistent since Amelia 2 (A2) motor (presented in Figure 3), one of its main parts was a composite (either fiberglass-epoxy or carbon-epoxy) casing with laminated stainless steel inserts. Each insert has a groove for retaining ring, locking the aft closure and the nozzle. Inside the casing, a layer of thermal insulation made of paper-phenolic composite was placed. The nozzle is made of the same composite material, with additional graphite insert to secure the throat. On the outer surface an aluminium ring is glued to the nozzle body to support the transfer of loads to retaining ring. The aft closure and the nozzle are sealed with two O-rings. Described design served as a baseline for each construction of solid rocket motor and later hybrid engine combustion chamber.

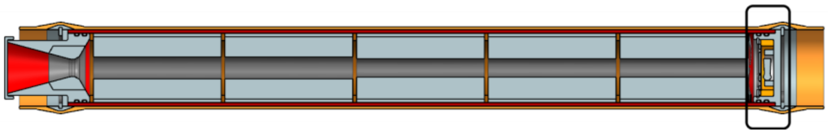

Figure 3 Cross-sectional view of A2 motor CAD model, with highlighted igniter location

Motors used in the first four rockets utilised the same igniter in design, only scaled in size to fit to the engine diameter. Its location in the motor is shown in Figure 3 while the construction is presented in Figure 4. The aft closure of the motor was used as the casing of the igniter, which stored the charge material, separated from the walls of closure with paper-phenolic insulation bushing. On top of this bushing, a steel sieve element was placed and secured with a retaining ring fitted into groove made in aft closure. The sieve was covered with tape or foil, to prevent the powder particles from falling out before ignition. The primer was glued to the closure and its wire was threaded through sieve's hole and went through the length of the motor. To allow pressure to buildup after ignition, the nozzle exit was closed with an aluminium cap glued to the outer surface of nozzle body, as can be seen on the Figure 3. To let the primer cable out of the motor, a hole through the cap was made, sealed with a layer of epoxy glue.

Ignition charge composition varied between motors. For A2 motor 1 g of black powder was mixed with 1 g of magnesium; H1 motor charge consisted of 15 g of black powder. In TuCAN motor the ignition charge was divided into two separate stages, the first one made of 4 g black powder, the second one of 12,5 g black powder mixed with 12,5 g $BKNO_3$.

DOI: 10.13009/EUCASS2025-118

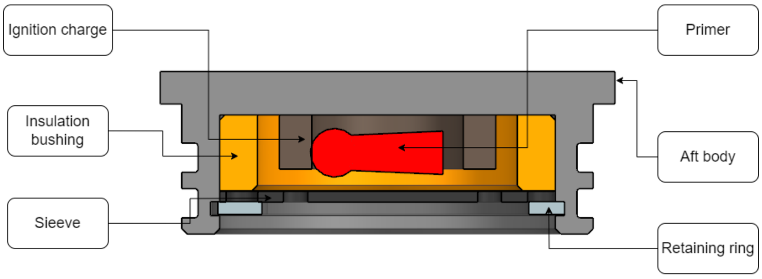

Figure 4 Cross sectional view of an igniter assembly CAD model

The main advantages of the presented igniter design were its simplicity, scalability and ease of assembly. The same design could be adjusted to A2 motor (42 mm diameter), H1 motor (100 mm diameter) or TuCAN (135 mm diameter), by simply scaling the diameters of components. However, it was not without its defects. Using the aft closure as igniter casing and closing the nozzle with glued cap meant that fully integrated motor was in armed state and had neither reliable nor safe method of disassembly. This posed a problem in motor transport and in case of launch abort. The second drawback of this design was the inefficiency of black powder particles scatter into the propellant grain through the sieve's holes (especially in smaller diameter motors). The combustion product particles tended to block the sieve's holes and after the motor disassembly large amounts of ignition charge remains were found in the aft closure.

Although the gluing of nozzle cap to the nozzle body was quick and simplified the assembly process, the strength of the adhesive joint depended on the gluing process conditions and pressure build-up before the cap separation was unique for each test. After a few failed launch attempts of different motors, a suspicion on the nozzle cap detaching too soon arose. Therefore, an experimental study on the pressure necessary for the cap to shear off was performed. The test setup consisted of assembled motor without the propellant, instead filled with water which was pressurized by an external pump. The results are presented in Table 1.

Table 1 Results of cap detach pressure tests

Attempt number	Maximum pressure [bar]	Notes
1	3.00	Joint width 3.5 mm
2	4.81	Joint width 3.5 mm
3	5.28	Joint width 3.5 mm[a]
4	4.34	Joint width 3,5 mm
5	15.6	Joint width 10 mm

[a]Used epoxy glue instead of cyanoacrylate

Results proved that the detach pressure increases with width of the glued joint, nevertheless for the same joint width the pressure is inconsistent. However, the nozzle body design limited the possible methods to attach the cap of the nozzle. The proposed alternative to the aft closure nozzle was to place the ignition charge in a body blocking the divergent part of the nozzle. This solution was utilised in motors of the Grot rocket and modified A2 rocket motor.

Although Grot motor design was adopted from TuCAN rocket motor, its igniter was redesigned, with aim to reduce the ignition delay. The igniter (presented in Figure 5) consisted of aluminium end body in conical shape, which was fitted to divergent part of the nozzle and a steel igniter casing with external thread to connect to the end body. Inside the casing an ignition charge, made of 30 g of KNO_3 formed into BATES type grain, was placed, covered with cardboard partition. Last part of the igniter assembly was a rubber tube, which extended forward from the igniter casing, to protect the nozzle throat from the combustion products and to direct the combustion products into grain inner channel. The reason behind this was a concern that ignition from front surface of the grain would cause a local increase in pressure high enough to push the igniter out. The igniter was mounted the same way as previously the cap was, by gluing it to the nozzle conical surface. However, the gluing area was increased, thus increasing the pressure at which the connection broke. This igniter was fired twice, successfully igniting the propellant in static fire and flight test, but no data regarding achieved ignition pressure was acquired from those tests.

DOI: 10.13009/EUCASS2025-118

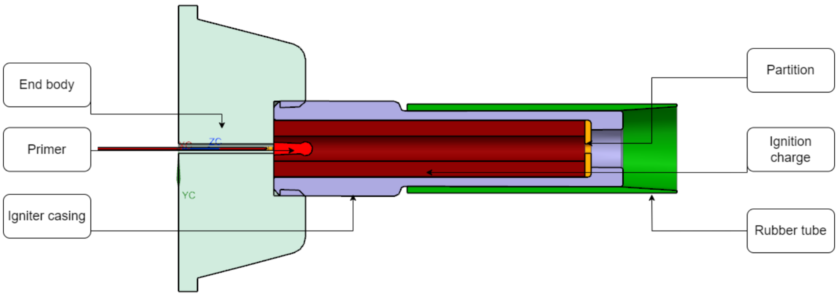

Figure 5 Cross sectional view of the Grot motor igniter assembly

Further plans of Grot [2] rocket development presumed a three-stage design, with two boosters utilising the same motor as in the first iteration of the project. To initiate the second stage in flight, the igniter needed to be modified. That is why the igniter was moved from the nozzle into the motor aft end. Newly designed igniter, displayed in Figure 6, consisted of a steel casing body with flange and space to store the ignition charge, closed off with a 3D printed cover. Igniter was connected to the aft closure by a set of screws. To seal the connection between the igniter and aft closure, a single O-ring was used. Primer wire was led through a hole in the back of the body. To seal the hole, the back of the casing was filled with resin.

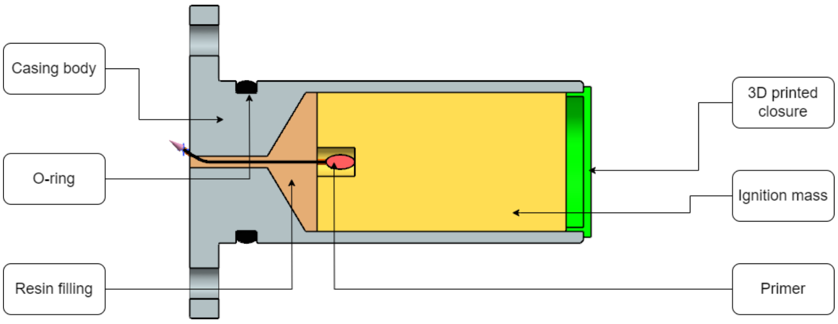

Figure 6 Cross sectional view of the Grot 2 motor igniter assembly

A single test static firing of this igniter was performed, due to limited access to test chamber in which test took place. In Figure 7 graph of pressure in function of time obtained in this test is presented. A maximum pressure achieved from burning mixture of 3,76 g of black and 4,89 g of nitrocellulose powder was equal to 3,55 MPa. Ignition delay was estimated equal to 40 ms. Pressure graph from test chamber was rescaled to Grot motor combustion chamber, multiplying it by ratio of test chamber to combustion chamber volume. Scaled pressure maximum is equal to 3.06 MPa.

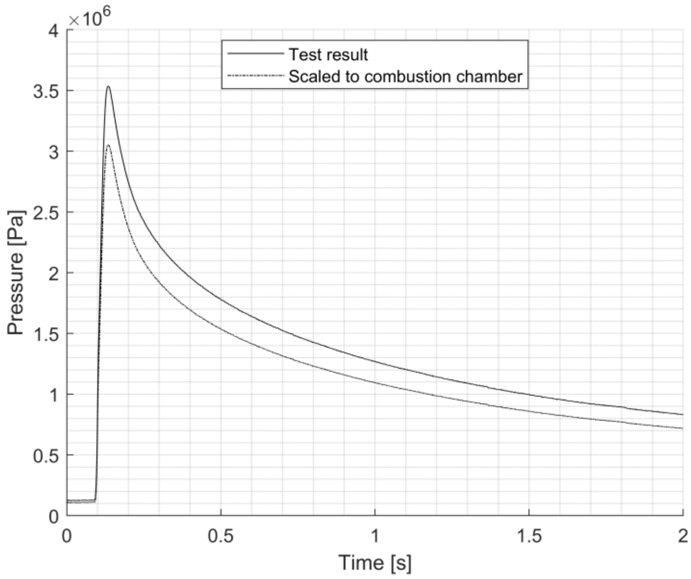

Figure 7 Pressure curve obtained during Grot second iteration igniter test

DOI: 10.13009/EUCASS2025-118

For the modified A2 motor two subsequent nozzle mounted igniters were designed from the course of recent hot fire and flight test campaigns. Due to the A2 motor being a much smaller device which is more frequently used, the simplicity and availability of the ignition materials was bigger factor in their selection than their performance. As a result, the single charge black powder-based design was adopted for both iterations.

The first iteration of the nozzle igniter had used a conical surface as a gluing interface to the nozzle, acting as a nozzle cup. The cup ejection pressure was greater compared to the previous design due to large, glued surface of a nozzle cup compared to the area which pressure acted on the igniter, just like in the Grot nozzle igniter. Ignition charge was placed inside the volume at the end of the cone with primer wire being sealed with rapid epoxy glue. To close off the ignition charge a packing tape was used.

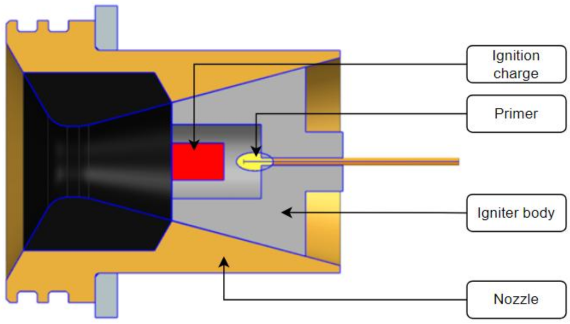

Figure 8 Cross sectional view of the A2 motor igniter first iteration assembly inside nozzle

This iteration was used for conducting 4 motor firings through the course of a static fire test and three FOK 2 rocket launches, where the ignition delays obtained from static and flight tests are shown in Table 2 with obtained effective total impulses of the each motor, measured from when each motor reached 10% of maximum thrust from test 1 (the weight of the rocket) until the end of its operation. As there is no pressure measurement in combustion chamber of this engine, ignition delay is estimated from time-lapse analysis of recorded video of nozzle exit, where delay is calculated as a time interval between the igniter ejection and the appearance of visible flame from the nozzle exit.

From the test data in Table 2 it is clearly seen that the ignition delay varied greatly across multiple firings where the gluing connection, with the charge being placed in a nozzle has resulted in the igniter detaching prematurely. Additionally, the tip of the igniter is placed before the nozzle throat and has larger diameter than the nozzle throat itself, which could lead to appearance of a region where pressure was significantly higher than the nozzle pressure. During test number 3, with the largest delay time, the obtained total impulse is also greatly lower than the performance in other tests.

Table 2 A2 motor nozzle igniter test data

Test no.	*Igniter iteration no.*	*Ignition delay (±0.1s)*	*Obtained total impulse to theoretical ratio ±5%)*
1[a]	*1*	- [c]	*97*
2[b]	*1*	*0.75*	*94*
3[b]	*1*	*1.7*	*80*
4[b]	*2*	*0.4*	*94*
5[a]	*2*	*0.6*	*Not measured*
6[b]	*2*	- [c]	*Not measured*

[a]Static fire test

[b]Flight test, motor total impulse data extracted from rocket onboard IMU

[c]Too short to be measurable with camera framerate

This led to the design and introduction of the new variant of the nozzle igniter which has consisted of two distinct parts: the conical interface to the nozzle extending to the nozzle throat, and a back section connected with the thread where the igniter charge was placed. The design of the igniter allowed for a compact fitting of much greater possible amount of black powder of maximum of about 3 grams in case more igniter volume would be needed, while fitting inside nozzle divergent section. During its use, however a filling part was implemented to limit the amount of charge due to the concerns about igniter detaching too early before ignition. The use of the two igniter parts allowed also for safer disarming of the motor in case of launch abort.

DOI: 10.13009/EUCASS2025-118

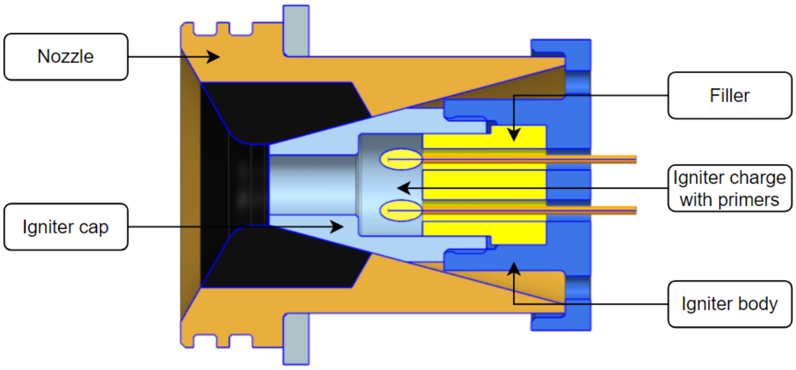

Figure 9 Cross sectional view of the A2 motor nozzle igniter first iteration assembly

In total, 3 tests using second iteration of the igniter were performed with results shown in Table 2. This iteration of the igniter yielded much more predictable ignition delay of 0.33±*0.3s* than the first iteration. However, the gluing connection of the igniter to the nozzle still did not allow for consistent motor ignition, and the igniter needed to be glued on launch site increasing the time needed for rocket preparation for flight.

For the next iterations of FOK 2 rocket igniters and motors which are being currently developed the changes to the ignition systems are planned, which consist of housing ignition charge in a separate casing threaded in to part mounted on motor nozzle, preferably with a non-glued connection.

5. Igniters of hybrid rocket engines

In the Association's first hybrid motor, called the Basilisk, ignition system consisted of small amount of rocket candy, which was glued on top of the solid fuel grain in a 3D-printed basket. Charge was positioned to be in the centre of the middle channel of the wagon-wheel type grain. Charge itself was formed by 3D printed body into end-burning grain (mass between 4 to 5 g) and its surface was covered in black powder (1 g layer) to increase ignition regularity over the face (see Figure 10). However, the use of rocket candy in this case resulted in the generation of a large number of burning particles that aided the ignition process, but due to the orientation of the igniter in the chamber, increased the risk of glowing solid particles getting behind the injection plate. Such an event also led to a single engine failure during a static running test due to oxidiser thermal decomposition.

It was therefore decided to use a black powder-based igniter that could further direct the generated stream of hot gases and hot particles towards the aft-end surface of the grain (see Figure 10). In this way, it was desired to reduce the aforementioned risk of spontaneous oxidiser decomposition. The use of black powder also based on experience with solid propellant motors and seemed to be a much more reliable and reproducible solution. Unfortunately, it proved to be ineffective due to the high combustion dynamics of black powder. As a result of the rapid build-up of pressure in the combustion chamber, which was much faster than observed while using rocket candy-based igniters, the nozzle plug ruptured rapidly, which released the powder combustion products before it had time to transfer heat to the grain surface. After unsuccessful engine static test using this igniter configuration, the previous design was reverted, while shielding the injection plate to avoid a repeat of the aforementioned failure.

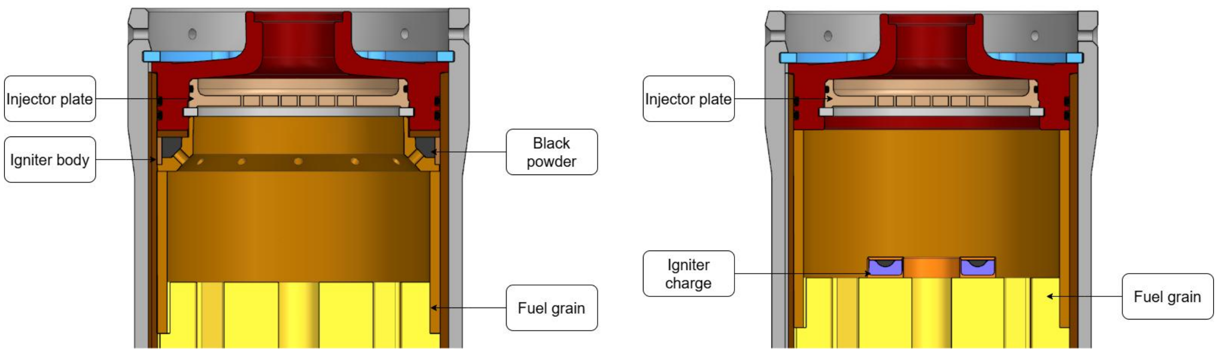

Figure 10 Cross-section view of two iterations of Basilisk hybrid engine igniter, potassium-sugar propellant based (right) and black powder based (left)

DOI: 10.13009/EUCASS2025-118

A several test firings of both igniters were performed to confirm repeatability of their operation. Test setup consisted of combustion chamber with grain mock-up, to simulate the free combustion chamber volume. The ignition charge was initiated by two primers, and the pressure was measured by sensor located in engine plug [4]. Unfortunately, due to low probing frequency, the pressure curve obtained during black powder-based igniter tests could not be accurately measured. The pressure curve since charge activation obtained during potassium sugar charge test is presented on Figure 11.

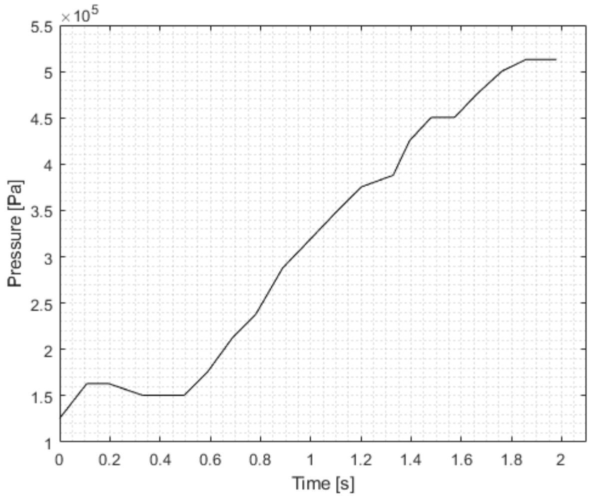

Figure 11 Pressure curve obtained during potassium sugar igniter charge test

At the beginning of Aurora hybrid rocket motor used in Twardowsky 2 rocket design, it was decided to use a similar ignitions system as in its predecessor. The initial design involved a small, 9 g charge of aluminium powder-infused rocket candy (based on sugar and potassium nitrate), formed into uniform cylinder in an end-burner configuration. Aluminium powder was included in the propellant mix, to raise igniter gasses temperature and propellant regression rate, which was a conclusion drawn from first hybrid igniter tests. A study was performed to estimate proper mass concentration. The propellant charge was meant to be initiated by black powder charge stored in 3D printed cylindrical igniter cup, which was ignited by electrical fuse. The rocket candy charge was formed into a uniform cylinder and used in an end-burn configuration. It was stored near the forward end of the fuel grain, embedded in a steel casing, installed in injection plate. The assembled igniter is presented in Figure 12.

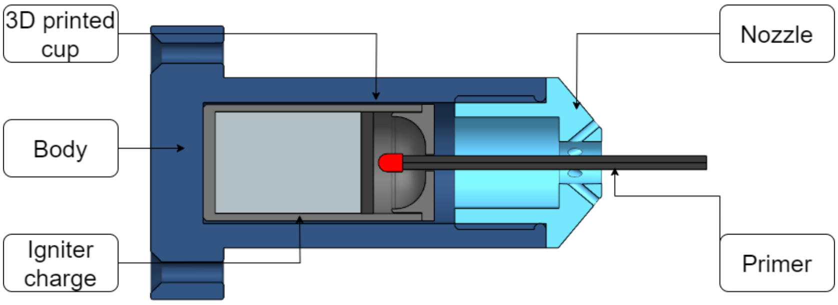

Figure 12 Cross-section of Aurora igniter assembly

For proper aluminium powder inclusion percentage choice, test campaign was conducted for test samples with aluminium mass concentration varying from 2 to 16% by 2%, three samples for each concentration. During the initial testing phase of such a selected ignition charge, significant difficulties were encountered in achieving its ignition. Such a phenomenon could have arisen for several reasons. Firstly, pure aluminium has a high tendency to react with atmospheric oxygen to form aluminium oxides [25], which require the supply of high energy to achieve their gasification. Such an effect could have occurred on the surface of a charge stored for a long time. In addition, it is suspected that the hot combustion products of the igniter initiator (in the form of a black powder charge) did not manage to transfer sufficient heat to the surface of the candy before leaving the igniter chamber. With the cigarette geometry of the candy grain, there was no flow of these gases along the grain channel, which would have allowed them to transfer a sufficient amount of heat to the surface of the grain. Due to failure to ignite rocket candy during the static igniter test, the geometry of igniter charge was changed to single circular channel configuration and an additional electrical fuse was added.

DOI: 10.13009/EUCASS2025-118

Subsequent tests performed with designated combustion chamber showed that due to a lot of aluminium residues, pressure achieved was non-satisfactory, as the measured 3 bar (attempt number 2 in Table 3) did not meet the expected design pressure of 10 bar. Apparently, either not enough aluminium entered the combustion reaction with rocket candy, or the combustion products have gone a recombination process, forming solid slug (presented in Figure 13). Its influence on combustion temperature was minimal, additionally limiting the mass of gaseous products created during ignition charge combustion, therefore lowering the pressure build-up. An additional test was performed with use of commercial solid propellant engine, based on a similar-in-composition propellant (attempt number 3 Table 3), to determine, whether the quality of self casted propellant had the effect on igniter performance. However, difference in results was not satisfying and required further igniter modifications.

Figure 13 Slug deposited at the igniter nozzle (left), visco fuse glued on top of the grain (right)

As additional energy source, to increase the pressure during combustion and transfer more heat directly to grain surface, a layer of visco fuse, glued directly to forward face of the fuel grain (see Figure 13), was added. About 3 meters of fuse have been used, which corresponds to 10.8 g of black powder. This solution was designed to deliver the large amount of heat produced by the products of fuse combustion directly to the grain surface. In addition, this configuration of the ignition system makes the ignition process independent of the hard-to-predict process of heat supply by the small burning particles of rocket candy produced by the previously used igniter integrated with the injector plate. Lastly, using fuse as igniter allows for better adjustability, as the amount of fuse glued on top of the grain surface can be more easily increased or decreased, basing on the test results.

Similar tests with combustion chamber proved this type of ignition raises pressure inside of combustion chamber to satisfactory level and, thanks to being glued directly to the fuel grain easily decomposes it. Ultimately, it was used in the successful hot-fire test of the whole rocket engine and is the designated ignition method for the rocket.

In Table 3 a summary of Aurora engine ignition system tests is presented, with comparison of maximum pressure obtained in combustion and time delay between the signal to primer and maximum pressure reached. A comparison of pressure in function of time is presented in Figure 14.

Table 3 Summary of Aurora engine ignition system tests

Test no.	**Maximum pressure [bar]**	**Delay of maximum pressure [±0.1s]**	**Implementation**
0[a]	No ignition	No ignition	
1[b]	-	-	BATES grain charge, double primer configuration
2[c]	2.8	1.3	
3[d]	3.5	1.7	
4[e]	-	-	new charge composition
5[f]	4.3	0.9	abandonment of aluminium addition
6	7.7	1.7	configuration with a coiled length of visco fuse
7	6.7	1.3	
8[g]	-	-	
9[h]	-	-	

DOI: 10.13009/EUCASS2025-118

[a]Unsuccessful; the old configuration – end-burning grain charge, aluminium addition (4%), black powder on the top, one primer
[b]No measurement – ignition test; 4% aluminium
[c]4% aluminium
[d]The only commercial charge test
[e]No measurement – ignition test
[f]The only configuration with no black powder
[g]No measurement – successful ignition test after charge prolonged exposure to low temperatures
[h]Successful hot fire test; uncertain pressure measurement

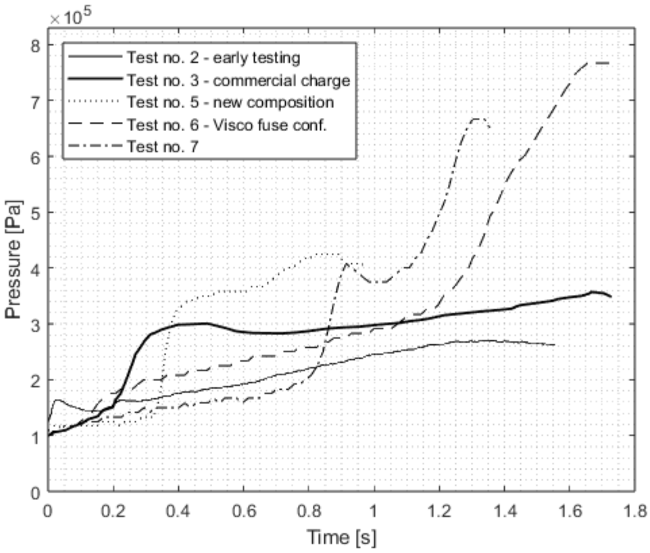

Figure 14 Pressure curves obtained during Aurora engine ignition system test campaign

During the test campaign of the Aurora hybrid rocket engine igniter, the aluminium-enriched compositions of potassium sugar-based propellants were utilized for the first time in the Association. However, this solution proved to be unsuccessful due to the inability to achieve full combustion of the material. It is possible that more thorough research into metallic additives for this type of composition would have allowed the development of a more efficient material that would have allowed higher combustion chamber pressures to be achieved. Finally, the use of visco fuse as an ignition material in direct contact with the surface of the grain allowed to achieve adequate ignition conditions, indicating the efficiency combined with the great simplicity and scalability of this solution.

6. Summary

Within 16 years of sounding rockets development in Students' Space Association various configurations of ignition systems for solid rocket motors and hybrid rocket engines have been designed and verified experimentally. Key designs have been described in detail, with highlighted advantages and disadvantages and test results. The most thorough test campaign of ignition system for Aurora hybrid engine was presented, with steps undertaken to obtain final igniter configuration, successfully implemented in motor first hot fire test.

Acknowledgements

Participation of authors of this paper in EUCASS 2025 was funded by the Polish Ministry of Science and Higher Education as part of *Wsparcie studentów w zakresie podniesienia ich kompetencji i umiejętności* programme. Development of Aurora hybrid propulsion system was supported by the Ministry of Science and Higher Education from *Studenckie koła naukowe tworzą innowacje 4.0* programme.
The solid propellant motors used a propellant obtained thanks to the contribution of the Division of the High Energy Materials of Chemical Faculty at Warsaw University of Technology, and the Łukasiewicz - Institute of Industrial Organic Chemistry.

DOI: 10.13009/EUCASS2025-118

References

[1] P. Wolański, M. Urbanowicz, and J. Pomierny, PW-Sat in Orbit, *Acad. Mag. Pol. Acad. Sci.*, vol. Nr 1 (33), pp. 24–27, 2012.

[2] S. Małecki *et al.*, The Challenges of Designing a Student Sounding Rocket For a 100 km Apogee, presented at the 73rd International Astronautical Congress, Paris, France, Aug. 2022.

[3] A. Okniński, The Development of the Small Sounding Rocket Program, presented at the 64th International Astronautical Congress, Beijing, China, Sep. 2013.

[4] M. Dzik, B. Hyży, D. Legutko, P. Chernenko, A. Kwitek, and J. Czerniej, Course and challenges of flight qualification test campaign of the students' hybrid rocket engine, presented at the 74th International Astronautical Congress, Baku, Azerbaijan, Oct. 2023.

[5] K. Szalkowski, M. Kret, J. Chrostowski, M. Sochacki, and M. Banaszak, Design and structural analysis of low-cost modular rocket engine test stand, presented at the 75th International Astronautical Congress, Milan, Italy, Oct. 2024.

[6] L. d'Agostino, L. Biagioni, and G. Lamberti, An ignition transient model for solid propellant rocket motors, in *37th Joint Propulsion Conference and Exhibit*, American Institute of Aeronautics and Astronautics. doi: 10.2514/6.2001-3449.

[7] O. Orlandi, F. Fourmeaux, and J. Dupays, Ignition Study at Small-Scale Solid Rocket Motor, in *EUCASS 2019*, Madrid, Spain, Jul. 2019. doi: 10.13009/EUCASS2019-757.

[8] S. Gallier, A. Ferrand, and M. Plaud, Three-dimensional simulations of ignition of composite solid propellants, *Combust. Flame*, vol. 173, pp. 2–15, Nov. 2016, doi: 10.1016/j.combustflame.2016.07.012.

[9] J. A. Keller, A. D. Baer, and N. W. Ryan, Ignition of ammonium perchlorate composite propellants by convective heating., *AIAA J.*, vol. 4, no. 8, pp. 1358–1365, 1966, doi: 10.2514/3.3678.

[10] B. L. Hicks, Theory of Ignition Considered as a Thermal Reaction, *J. Chem. Phys.*, vol. 22, no. 3, pp. 414–429, Mar. 1954, doi: 10.1063/1.1740083.

[11] Solid rocket motor igniters., NASA, Space Vehicle Design Criteria NASA SP-8051, Mar. 1971.

[12] E. W. Price, H. H. Bradley, L. Dehorlty, and M. M. Iblricu, Theory of Ignition of Solid Propellants.

[13] R. F. McAlevy, P. L. Cowan, and M. Summerfield, The Ignition Mechanism of Composite Solid Propellants, *Prog. Astronaut. Rocket.*, vol. 1, 1960.

[14] C. E. Hermance, R. Shinnar, and M. Summerfield, Ignition of an evaporating fuel in a hot, stagnant gas containing an oxidizer., Sep. 1965.

[15] R. Anderson, R. S. Brown, C. T. Thompson, and R. W. Ebeling, Theory of hypergolic ignition of solid propellants, presented at the Heterogeneous Combustion Conference, Palm Beach, Florida, USA: American Institute of Aeronautics and Astronautics, Dec. 1963.

[16] H. Tian, X. Li, and G. Cai, Ignition theory investigation and experimental research on hybrid rocket motor, *Aerosp. Sci. Technol.*, vol. 42, pp. 334–341, Apr. 2015, doi: 10.1016/j.ast.2015.01.015.

[17] F. M. Owis, Design and testing of the ignition system for hybrid Rocket motor, *Int. Conf. Aerosp. Sci. Aviat. Technol.*, vol. 11, no. ASAT Conference, 17-19 May 2005, pp. 427–440, May 2011, doi: 10.21608/asat.2011.27161.

[18] M. A. Karabeyoglu, Transient combustion in hybrid rockets, Ph.D. thesis, Stanford University, California, USA, 1998. Accessed: Jun. 06, 2025. [Online]. Available: https://ui.adsabs.harvard.edu/abs/1998PhDT.......265K

[19] H. G. Landau, Heat conduction in a melting solid, *Q. Appl. Math.*, vol. 8, no. 1, pp. 81–94, Apr. 1950, doi: 10.1090/qam/33441.

[20] M. Tomporowski *et al.*, Development and validation of rocket motor simulation software, presented at the 75th International Aeronautical Congress, Oct. 2025. doi: https://doi.org/10.52202/078371-0116.

[21] T. L. Davis, *The Chemistry of Powder and Explosives*. Sevenoaks : San Francsico: Pickle Partners Publishing INscribe Digital [Distributor], 2016.

[22] L. Yang, Effects of Fuel Particle Size and Impurity on Solid-to-Solid Pyrotechnic Reaction Rate, in *47th AIAA/ASME/SAE/ASEE Joint Propulsion Conference & Exhibit*, American Institute of Aeronautics and Astronautics. Accessed: Jun. 08, 2025. [Online]. Available: https://arc.aiaa.org/doi/abs/10.2514/6.2011-5581

[23] A. B. Ray, Incendiaries in Modern Warfare., *J. Ind. Eng. Chem.*, vol. 13, no. 7, pp. 641–646, 1921, doi: 10.1021/ie50139a030.

[24] D. A. Reese, D. M. Wright, and S. F. Son, CuO/Al Thermites for Solid Rocket Motor Ignition, *J. Propuls. Power*, vol. 29, no. 5, pp. 1194–1199, 2013, doi: 10.2514/1.B34771.

[25] L. Huang *et al.*, The Mechanism of Oxide Growth on Pure Aluminum in Ultra-High-Temperature Steam, *Metals*, vol. 12, no. 6, Art. no. 6, Jun. 2022, doi: 10.3390/met12061049.